LETTERS
PUBLISHED ONLINE: 27 MARCH 2011 | DOI: 10.1038/NGEO1110
nature geoscience

Absence of remotely triggered large earthquakes beyond the mainshock region

Tom Parsons[1]* and Aaron A. Velasco[2]

Large earthquakes are known to trigger earthquakes elsewhere. Damaging large aftershocks occur close to the mainshock and microearthquakes are triggered by passing seismic waves at significant distances from the mainshock[1–6]. It is unclear, however, whether bigger, more damaging earthquakes are routinely triggered at distances far from the mainshock, heightening the global seismic hazard after every large earthquake. Here we assemble a catalogue of all possible earthquakes greater than *M* 5 that might have been triggered by every *M* 7 or larger mainshock during the past 30 years. We compare the timing of earthquakes greater than *M* 5 with the temporal and spatial passage of surface waves generated by large earthquakes using a complete worldwide catalogue. Whereas small earthquakes are triggered immediately during the passage of surface waves at all spatial ranges, we find no significant temporal association between surface-wave arrivals and larger earthquakes. We observe a significant increase in the rate of seismic activity at distances confined to within two to three rupture lengths of the mainshock. Thus, we conclude that the regional hazard of larger earthquakes is increased after a mainshock, but the global hazard is not.

Surface waves are usually the largest-amplitude arrivals on a seismogram, and they produce transient strain as they travel within Earth's crustal waveguide. Large ($M \geq 7$) earthquakes are known to trigger earthquakes[1–6] and other phenomena, such as non-volcanic tremor[7–11], at remote distances. Although remote earthquake triggering is seen in all tectonic settings[12], the mechanism of triggered earthquake failure remains unsolved. Thus far, the remotely triggered earthquakes we have associated with the onset of passing seismic waves have been small-magnitude ($M < 5$) events. However, what if each large mainshock raises the global rate of other large earthquakes? Should there be a worldwide alarm period of heightened earthquake probability? We turn to the 30-yr global catalogue to search for high-magnitude ($M > 5$) triggered earthquakes at all offsets following large ($M \geq 7$), shallow ($Z \leq 50$ km) earthquakes to see whether there are significant rate increases.

Our global earthquake catalogue is compiled from the Advanced National Seismic System and Global Seismograph Network. We find the minimum magnitude of completeness to range between coda magnitude (M_c) = 4.7 and $M_c = 5.1$, depending on the methods applied (Supplementary Fig. S1). We thus investigate $M > 5$ events throughout this study, which we define as earthquakes with catalogue listings of $M \geq 5.1$. As will be shown, we conducted tests with $M_c \geq 5.5$ and $M_c \geq 6.0$ without substantive change in result.

We identify links among large earthquakes by calculating earthquake density (number km^{-2}) for $5 < M < 7$ events in concentric radii measured from 205 $M \geq 7$ global earthquakes (1979–2009). We calculate earthquake density to normalize results calculated over the larger areas caused by increasing radii. We isolate the largest events ($M \geq 7$) for study as triggering mainshocks, leaving 25,222 potentially triggered $5 < M < 7$ events. We compute relative origin times and ranges of every $5 < M < 7$ catalogue event to each of the 205 $M \geq 7$ mainshocks. We then calculate before and after $5 < M < 7$ earthquake density (number km^{-2}) in bins ranging from 20 to 200 km width, and over 100 time intervals ranging from 30 s to 1 day (Fig. 1; see Methods).

We determine the significance of observed rate changes by establishing the global background rate of $5 < M < 7$ earthquakes over the time and distance ranges used in the study. The question we want to answer in establishing significance is, what are the mean and confidence bounds on the expected steady-state density of $5 < M < 7$ earthquakes as a function of distance from the $M \geq 7$ triggering event locations used in the study? This allows us to recognize anomalous rate changes at any distance range. For example, if we know the mean background rate in a given window of time as a function of distance from sources, we can compare it with the observed rate versus distance. Wherever or whenever the observed density is significantly higher than background, then we suspect triggering is happening. We examine many periods at random times throughout the 30-year catalogue to establish mean rates and confidence bounds (see Methods).

We search for triggered earthquakes that lie within and after time intervals containing surface-wave arrivals (Fig. 2), but find no significant $5 < M < 7$ earthquake rate increase coincident with surface-wave arrivals at any distance range on Earth in the past 30 years. This result is surprising because past studies[12], using just 15 mainshocks and spatially limited detection, identified ~1,500 $M \leq 3$ events that occurred within 15 min of the first surface-wave arrivals. Extrapolating with the Gutenberg–Richter relation between magnitude and frequency ($\log N = a - bM$, where N is the number of earthquakes and a and b are constants defining intercept and linear slope), we expect a minimum of ~70 $M > 5.0$ and ~25 $M > 6.0$ triggered earthquakes to have occurred above background rates within 15 min of surface-wave arrivals after 205 mainshocks over 30 yr.

We calculate the Gutenberg–Richter relation using the number of triggered detections for 15 large ($M > 7.0$) earthquakes[12]. If we assume that all of the detections recorded in the first 15 min were triggered events (~1,500) with maximum magnitude $M \leq 3.0$ and a b value of 1.0, we expect at least five $M > 5.0$ and two $M > 6.0$ triggered earthquakes should have occurred. If we assume $M < 2.0$ for all triggered events, the number of triggered earthquakes decreases to approximately two for $M > 5.0$ and 0.2 for $M > 6.0$ in 14 years previously studied[12]. In our case, we analyse data from a 30-year span, indicating that we should at minimum expect 4–10 $M > 5.0$ triggered events and 0–2 $M > 6.0$ triggered events. This is a lower bound estimate, because it is based only on 15 $M > 7.0$ earthquakes, and detections were spatially limited to events very

[1]US Geological Survey, MS-999, 345 Middlefield Rd, Menlo Park, California 94025, USA, [2]Department of Geological Sciences, University of Texas at El Paso, El Paso, Texas 79968-0555, USA. *e-mail: tparsons@usgs.gov.

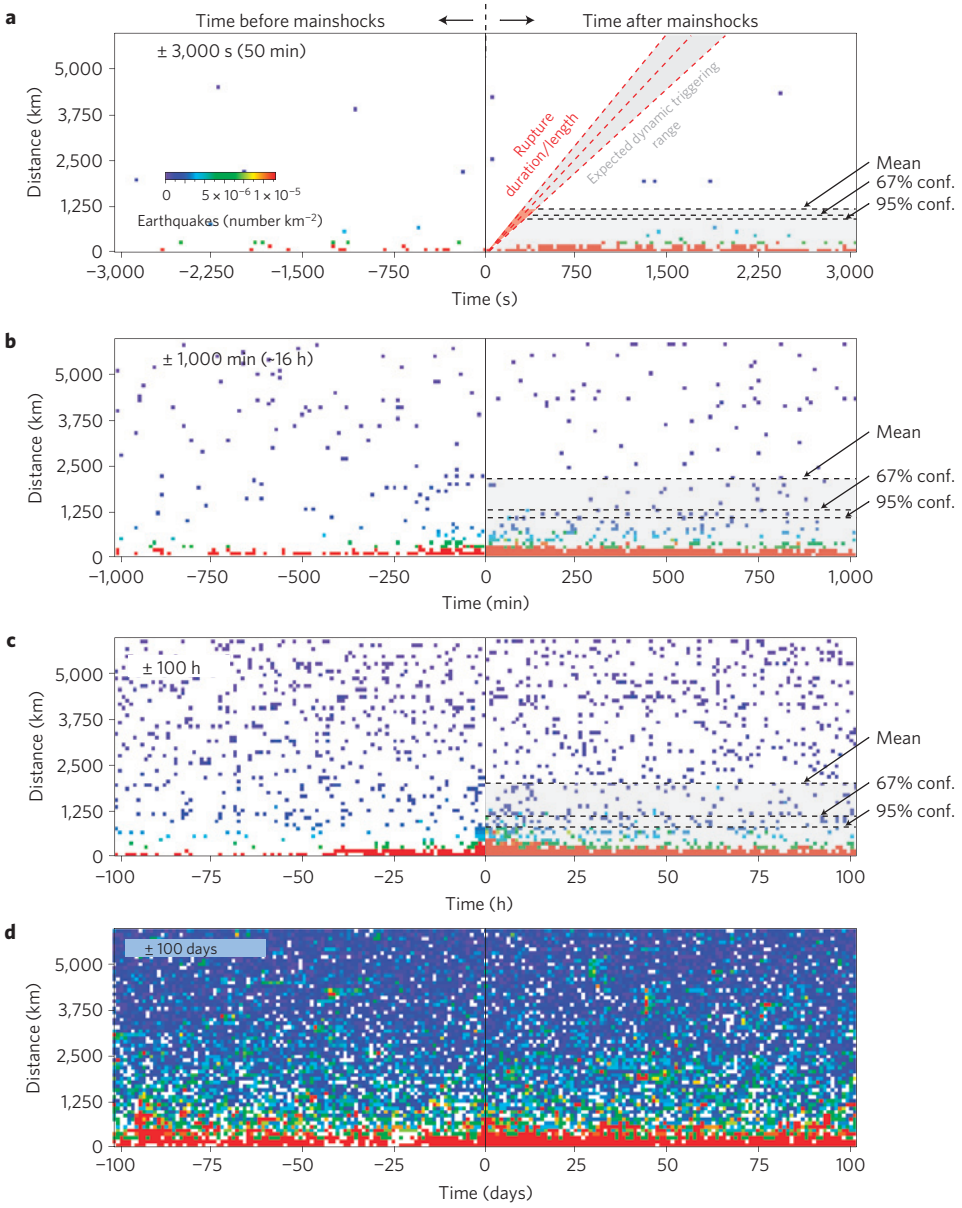

Figure 1 | Time and distance distribution (to 6,000 km) of large ($5 < M < 7$) aftershocks from 205 $M \geq 7$ mainshocks. a, Distribution for a 50-min period before and after triggers. The shaded region identifies the possible time and distance range of surface-wave arrivals. **b**–**d**, The same information as in **a**, but for a 1,000 min before and after period (~16 h; **b**), a ±100 h period (**c**) and a ±100 day interval (**d**). Rates in the before periods (especially in **c** and **d**) appear higher just before the trigger times ($t = 0$), indicating foreshocks.

near stations[12]. Extrapolating to 205 mainshocks, we arrive at the ~70 expected minimum number of $M > 5$ events.

Could the global network systematically be failing to detect any rate increases? For example, analysis of the Harvard central moment tensor (CMT) catalogue[13] indicates that 'several per cent or several tens of per cent of earthquakes' could be missing between 0.1 and 0.5 days after $M \geq 6.0$ earthquakes, although the reason for missing events is in part because moment tensor solutions are obtained by waveform inversion rather than phase arrival times used for hypocentre detection. In other words, criteria for inclusion of events into CMT catalogues are stricter than hypocentre catalogues that we use, and even these are at least partially complete above $M_c = 5.0$ during surface-wave arrivals. Furthermore, most missing events are located near mainshocks because it can be difficult to identify individual signals from numerous closely spaced events; we avoid this problem by using the global network to search for long-range event pairs that have significant travel-time separations.

Finally, we carried out the same analysis as shown in Fig. 2, but with higher completeness thresholds of $M_c = 5.5$ and $M_c = 6.0$ that are less likely to go undetected without any change in result (Supplementary Fig. S2).

We find evidence for delayed triggering of larger events that extends to ~1,000 km from mainshocks (Fig. 2); these events show different temporal and spatial reactions to external stressing when compared with $M < 5$ earthquakes, which can be triggered immediately at any distance by dynamic stresses imparted by passing surface waves[1–6,12]. Triggering of $5 < M < 7$ events is delayed by minutes to hours; we observe significant $5 < M < 7$ rate increases beginning within the first hour after surface-wave arrivals (Figs 2 and 3), and persisting for 20–30 h in the 300–1,000 km distance interval. This range is inferred to be at the far reach of static-stress changes[14–17], meaning these events could be triggered by dynamic or static processes. By extending the analysis time over hours and days past the trigger origin times, we see an Omori-law

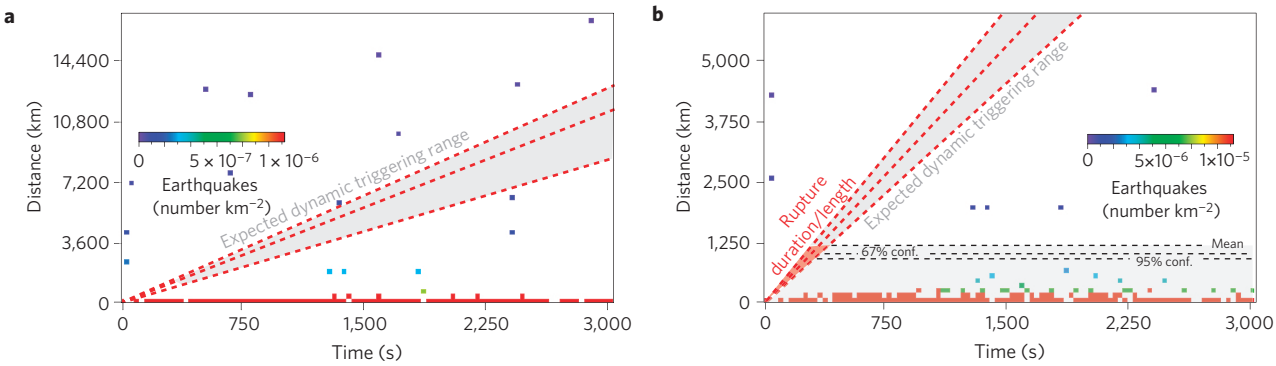

Figure 2 | Earthquake density (number km^{-2}) as a function of time and distance. The shaded region identifies the possible time and distance range of surface-wave arrivals. **a**, Compilation of the first 50 min of post-seismic time following 205 $M \geq 7.0$ earthquakes taken from 1979 to 2009 out to an 18,000 km offset from mainshocks. During that period, all $5 < M < 7$ triggered aftershocks were confined to regions near (≤1,000 km) mainshocks. No significant $M > 5.0$ rate increase can be attributed to coincident dynamic stresses caused by the passage of seismic arrivals (group velocity ranges 3.0–4.5 km s^{-1}). **b**, 50 min after mainshocks, to 6,000 km, with confidence bounds on the maximum significant range of $M > 5$ rate increase.

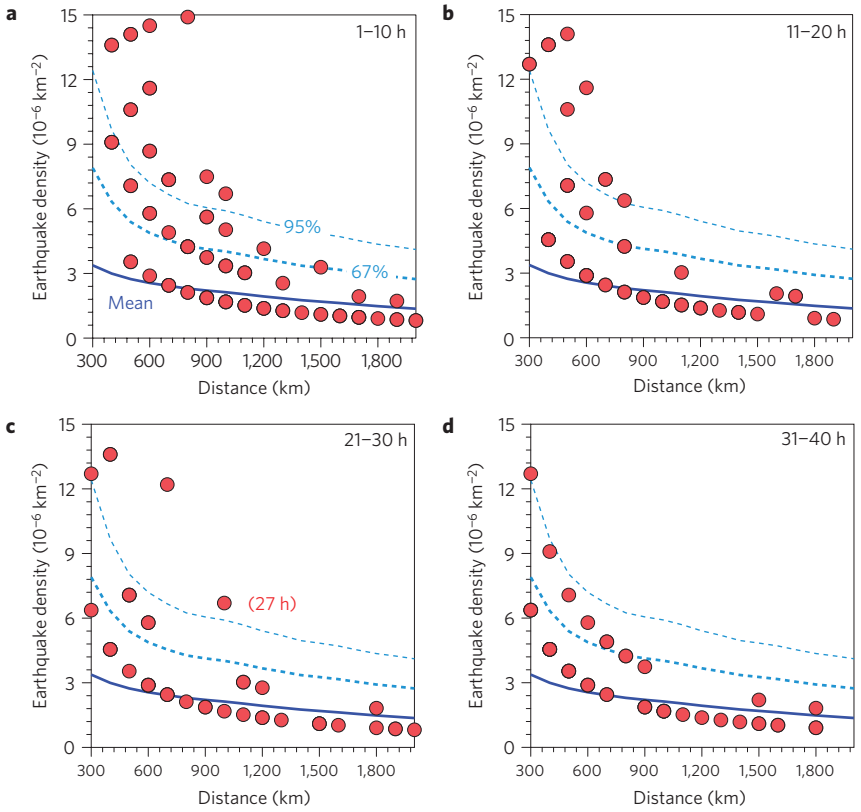

Figure 3 | Timing of global $5 < M < 7$ earthquake rate increase following $M \geq 7$ triggers at ≥300 km distances. The red dots show stacked $5 < M < 7$ rate-versus-distance pairings at 1-h intervals, and blue curves give mean and confidence on background $5 < M < 7$ rates. Rates return below 95% confidence bounds on background rates after 20–30 h. **a**–**d**, Results grouped for 1–10 h (**a**), 11–20 h (**b**), 21–30 h (**c**) and 31–40 h (**d**) after a mainshock. Note that rate increase persists for at least 20–30 h in the 300–1,000 km interval, and could be caused by static- or dynamic-stress changes.

rate increase and a return to background $5 < M < 7$ rates within about 30 h (Figs 1 and 3).

The <1,000-km maximum offset distance and temporal delay for larger earthquake triggering indicates dependence of the eventual magnitude of a triggered earthquake on stress-change amplitude and/or duration, and a different, slower nucleation process for larger earthquakes than smaller ones. We test amplitude/duration dependence by limiting the maximum magnitudes of triggering mainshocks, and note a clear impact on the maximum offset of triggered $5 < M < 7$ earthquakes (Fig. 4). In the first 50 min after mainshocks, 95% of triggered $5 < M < 7$ events occur within a 1,000 km offset when trigger magnitudes up to $M \leq 8.6$ are allowed. That range decreases to 400 km when trigger magnitude is limited to $M \leq 7.5$. Similar ranges are observed for longer intervals of 16 and 100 h (Fig. 4). Generally, the maximum observed distance extent of $M > 5$ earthquake triggering is limited to within ~2–3 mainshock rupture lengths.

Our results are empirical; we observe no significant short-term association between $M \geq 7$ and $5 < M < 7$ earthquakes at the global range during the past 30 yr. The possibility of diminished event detection exists during the passage of surface waves through the global network. However, at a minimum, our

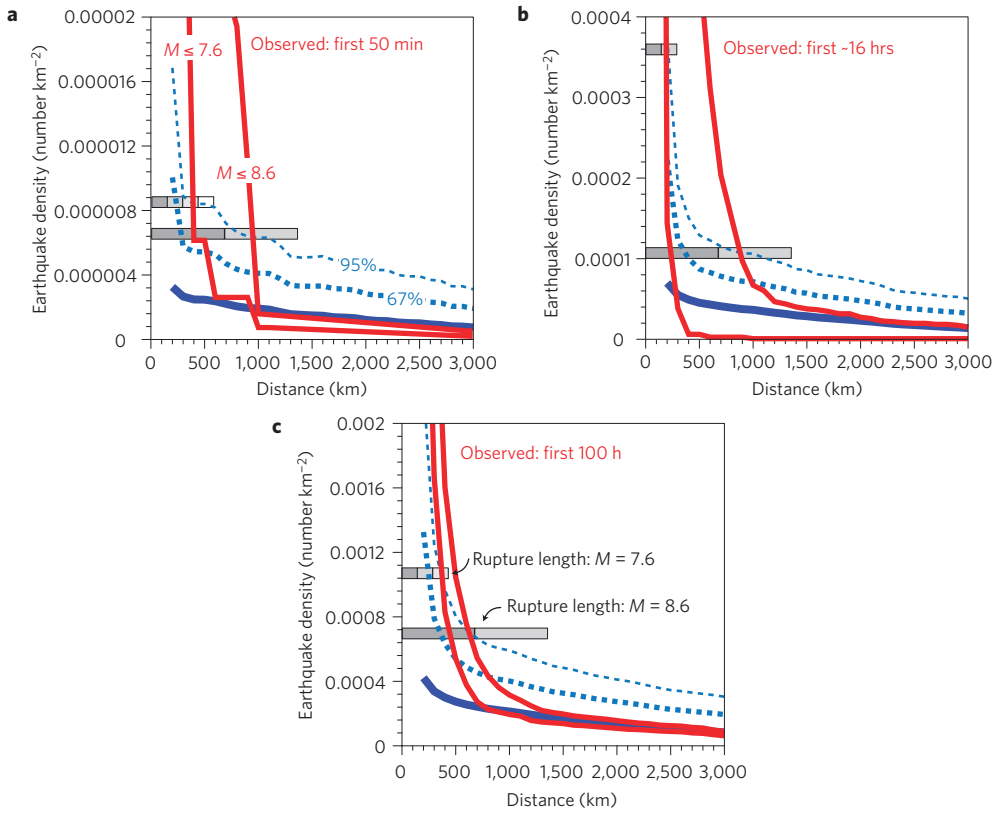

Figure 4 | Observed $5 < M < 7$ earthquake rate increase versus distance. The red curves show earthquake density versus distance from $M \leq 7.6$ and $M \leq 8.6$ mainshocks in different time intervals. **a**–**c**, Calculated rates following the first 50 min (**a**), the first 16 h (**b**) and the first 100 h (**c**) after a mainshock. Background mean rates and confidence bounds (blue curves) were developed from 100 calculations using the 205 $M \geq 7$ trigger locations, but with randomized times; background rates are higher at near ranges because earthquakes tend to cluster spatially on plate boundaries. Horizontal grey bars show increments of $M = 7.6$ and $M = 8.6$ rupture lengths; significant triggered rate increases are observed to maximum distances of two to three mainshock rupture lengths.

analysis shows that in the past 30 yr, there is no evidence for very large earthquakes promoting other very large earthquakes at a global scale, whereas such triggering is common near mainshocks over the same 30-yr period. If dynamic triggering of larger earthquakes at global distances is delayed by more than a few days, then such a rate increase is lost in the background rate where it cannot be detected readily.

Our results imply either a distinct nucleation process for larger earthquakes[18], or that triggering them requires a stronger, more sustained stress change than for smaller events; lower-magnitude earthquakes are triggered immediately by surface waves and persist at higher than background rates for less than 1 h (ref. 12). If cascading nucleation from small patches evolves into larger earthquakes, it must happen slowly because otherwise some percentage of smaller earthquakes triggered at >1,000 km distances would evolve into $5 < M < 7$ events, which has not happened simultaneously with passing surface waves in the past 30 years. The earliest onset of triggered $M > 5$ events begins ~200 s after the slowest surface waves have passed, but most are delayed by hours (Fig. 3).

Nucleation of triggered $5 < M < 7$ shocks seems to require a specific stress-change amplitude or duration threshold to be reached as evidenced by mainshock magnitude controls on maximum triggering range (Fig. 4), and correlations between large earthquake triggering and long-duration static-stress changes[14–17]. The physics of dynamic triggering probably represents complex dependencies[19] between faults (length and orientation), surface-wave stresses, pore fluids and aseismic transient slip, such that a larger nucleation area might require a greater amplitude and/or duration of stress change. Secondary triggering by static-stress transfer at remote distances[20] could partly explain a delayed response if smaller triggered earthquakes act as foreshocks to $M > 5$ events, but this process cannot explain the amplitude/distance dependence of $5 < M < 7$ triggering because smaller earthquakes are triggered at all ranges.

We conclude from global earthquake patterns over the past 30 years that there is no increased $M > 5$ earthquake hazard at distances beyond about 2–3 $M > 7$ mainshock rupture lengths. This means that rapid triggering of $5 < M < 7$ earthquakes occurs only within 1,000 km of the largest mainshocks, with 95% of those shocks occurring within 600 km.

Methods

Earthquake range binning. Through the course of the study, we experimented with a variety of distance and time increments. We adopt a 100-km-radius increment because this fully incorporates the maximum location uncertainty reported in the catalogue. Varying distance increments between 20 km up to 200 km does not result in any perceptible change in results. This is because for most of the distance range from sources ($r > 1{,}000$ km), there are very few earthquakes; most time–distance bins have zero or one event in them, causing distance discretization to have little effect on the results. A different effect is seen with changing time intervals. Background rates increase with greater intervals (Fig. 2); we note no significant change to our conclusions by lengthening intervals up to about one hour (Fig. 1c). For longer intervals, background events swamp any triggering signal we might observe (Fig. 1d).

Earthquake rate-change significance testing. Global earthquakes are not uniformly distributed, but instead mostly cluster spatially near plate boundaries, and temporally as aftershocks. We opt not to apply an aftershock declustering algorithm because of introduced uncertainties needed for global parameter choices. Instead, we use randomized origin times for mainshocks, but retain their original

positions. In this way we maintain spatial clustering related to tectonics, while taking advantage of the 30-yr duration of the catalogue to average out temporal clustering of aftershocks. This approach gives us a higher mean rate than a fully declustered catalogue because it includes aftershocks. However, a completely declustered background rate would be artificially low because there are usually one or more active aftershock sequences operating globally. Regardless, our primary result is independent of the background rate because we observe no $5 < M < 7$ events at all during surface-wave arrival times. For all of these reasons, we develop mean earthquake density versus distance, and density versus time from 100-each samples of the temporally randomized global $5 < M < 7$ catalogue for every distance and time interval used in the study. We calculate confidence bounds on the mean based on the variability across the 100 calculation sets.

Received 28 July 2010; accepted 14 February 2011; published online 27 March 2011

References

1. Hill, D. P. *et al*. Seismicity in the western United States remotely triggered by the M 7.4 Landers, California, earthquake of June 28, 1992. *Science* **260,** 1617–1623 (1993).
2. Brodsky, E. E., Karakostas, V. & Kanamori, H. A new observation of dynamically triggered regional seismicity: Earthquakes in Greece following the August, 1999 Izmit, Turkey earthquake. *Geophys. Res. Lett.* **27,** 2741–2744 (2000).
3. Kilb, D., Gomberg, J. & Bodin, P. Triggering of earthquake aftershocks by dynamic stresses. *Nature* **408,** 570–574 (2000).
4. Gomberg, J., Reasenberg, P., Bodin, P. & Harris, R. Earthquake triggering by transient seismic waves following the landers and hector mine, California earthquakes. *Nature* **411,** 462–466 (2001).
5. Gomberg, J., Bodin, P., Larson, K. & Dragert, H. Earthquake nucleation by transient deformations caused by the $M = 7.9$ Denali, Alaska, earthquake. *Nature* **427,** 621–624 (2004).
6. West, M., Sanchez, J. J. & McNutt, S. R. Periodically triggered seismicity at Mount Wrangell, Alaska, after the Sumatra earthquake. *Science* **308,** 1144–1146 (2005).
7. Miyazawa, M. & Mori, J. Detection of triggered deep low-frequency events from the 2003 Tokachi-oki earthquake. *Geophys. Res. Lett.* **32,** L10307 (2005).
8. Rubinstein, J. L. *et al*. Non-volcanic tremor driven by large transient shear stresses. *Nature* **448,** 579–582 (2007).
9. Miyazawa, M. & Brodsky, E. E. Deep low-frequency tremor that correlates with passing surface waves. *J. Geophys. Res.* **113,** B01307 (2008).
10. Peng, Z. & Chao, K. Non-volcanic tremor beneath the Central Range in Taiwan triggered by the 2001 Mw 7.8 Kunlun earthquake. *Geophys. J. Int.* **175,** 825–829 (2008).
11. Gomberg, J., Rubinstein, J. L., Peng, Z., Creager, K. C. & Vidale, J. E. Widespread triggering of non-volcanic tremor in California. *Science* **319,** 173 (2008).
12. Velasco, A. A., Hernandez, S., Parsons, T. & Pankow, K. The ubiquitous nature of dynamic triggering. *Nature Geosci.* **1,** 375–379 (2008).
13. Iwata, T. Low detection capability of global earthquakes after the occurrence of large earthquakes: Investigation of the Harvard CMT catalogue. *Geophys. J. Int.* **174,** 849–856 (2008).
14. Harris, R. A. Introduction to special section: Stress triggers, stress shadows, and implications for seismic hazard. *J. Geophys. Res.* **103,** 24347–24358 (1998).
15. Stein, R. S. The role of stress transfer in earthquake occurrence. *Nature* **402,** 605–609 (1999).
16. Freed, A. M. Earthquake triggering by static, dynamic, and postseismic stress transfer. *Annu. Rev. Earth Planet. Sci.* **33,** 335–367 (2005).
17. Parsons, T. Global Omori law decay of triggered earthquakes: Large aftershocks outside the classical aftershock zone. *J. Geophys. Res.* **107,** 2199 (2002).
18. Ellsworth, W. L. & Beroza, G. C. Seismic evidence for an earthquake nucleation phase. *Science* **268,** 851–855 (1995).
19. Hill, D. P. Dynamic stresses, Coulomb failure, and remote triggering. *Bull. Seismol. Soc. Am.* **98,** 66–92 (2008).
20. Ziv, A. What controls the spatial distribution of remote aftershocks? *Bull. Seismol. Soc. Am.* **96,** 2231–2241 (2006).

Acknowledgements

We thank E. Brodsky, R. Stein, S. Toda and N. van der Elst for critical comments on written and oral versions of this presentation.

Author contributions

T.P. and A.A.V. wrote the manuscript collaboratively. T.P. wrote the catalogue search and distance range codes. A.A.V. developed the concept of GSN waveform filtering for remote triggered earthquakes enabling a comparison of large and small events.

Additional information

The authors declare no competing financial interests. Supplementary information accompanies this paper on www.nature.com/naturegeoscience. Reprints and permissions information is available online at http://npg.nature.com/reprintsandpermissions. Correspondence and requests for materials should be addressed to T.P.

nature geoscience
SUPPLEMENTARY INFORMATION
DOI: 10.1038/NGEO1110

Supplementary Materials for: "No significant remote triggering observed for *M*>5 earthquakes" by Tom Parsons and Aaron A. Velasco

We assess the completeness of the 1979- 2009 shallow earthquake catalog using three methods, (1) the maximum curvature method of *Wiemer and Wyss* [2000], (2) the goodness-of-fit test [*Wiemer and Wyss*, 2000], and (3) the b-value stability test of *Cao and Gao* [2002] as modified by *Woessner and Weimer* [2005]. A minimum detection magnitude evaluation conducted midway through our catalog duration found the thresholds to be *Mc*=4.2 in the northern hemisphere, and *Mc*=4.6 in the southern hemisphere [*Ringdal*, 1986].

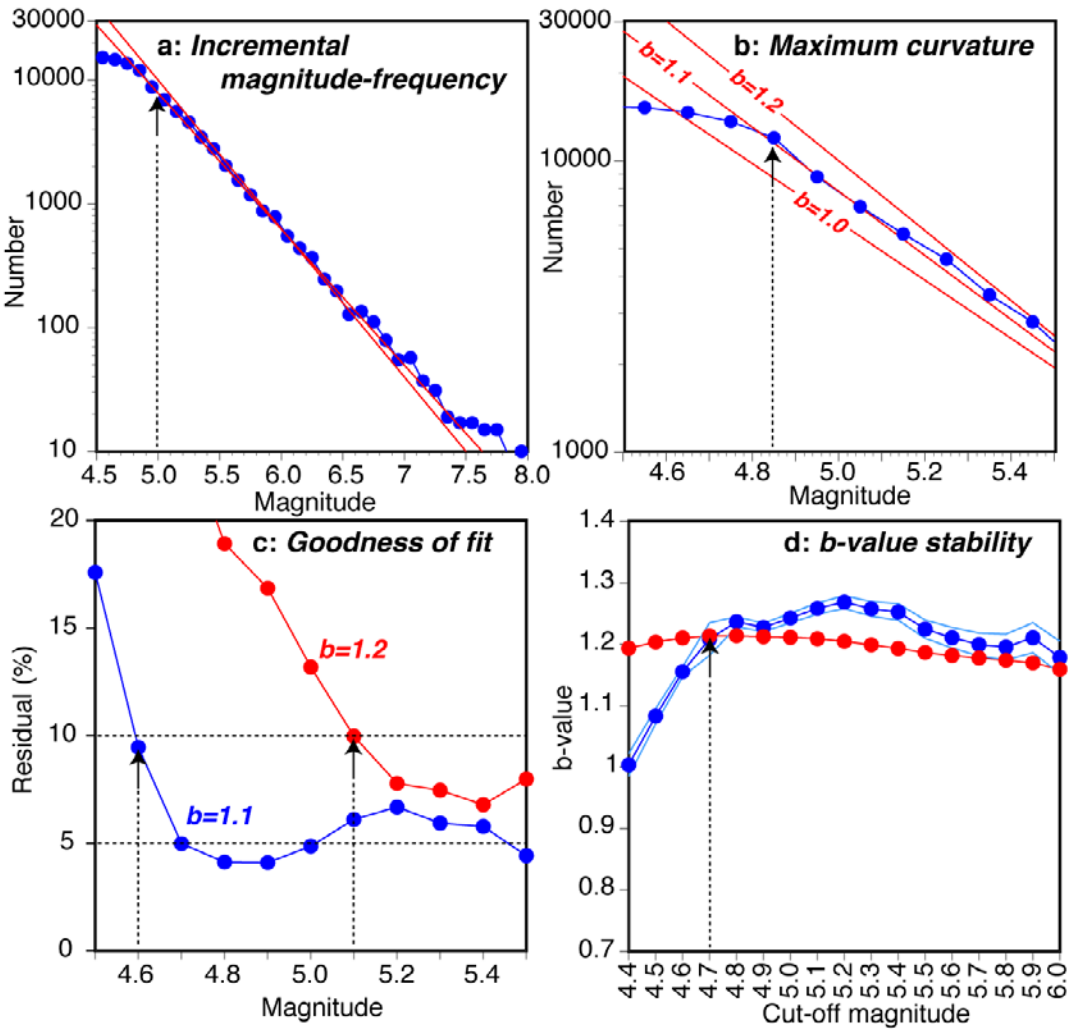

DOI: 10.1038/NGEO1110

Figure S1. Global Catalog completeness. a, Incremental magnitude-frequency plot of the 30-yr ANSS catalog that begins to roll off around *M*=5. The b-value of the whole catalog above M=5.0 is *b*=1.24 by maximum likelihood. In **b**, the maximum curvature method of *Wiemer and Wyss* [2000] is applied, and the magnitude of completeness (*Mc*) is estimated at *M*=4.85. In **c,** the goodness-of-fit method of *Wiemer and Wyss* [2000] is applied for *b*-values of *b*=1.1 and *b*=1.2, which results in estimates of *Mc* ranging from *M*=4.6 to *M*=5.1 (using the criterion that 90% of the data above *Mc* are fit are fit by the *b*-value model). In **d,** the b-value stability model of *Cao and Gao* [2002] is used with the criterion recommended by *Woessner and Wiemer* [2005] that the difference between b-value calculated above a cut-off magnitude (blue curve) and average b-value (red curve) be less than the calculation uncertainty [*Shi and Bolt*, 1982]. This method gives *Mc*=4.7.

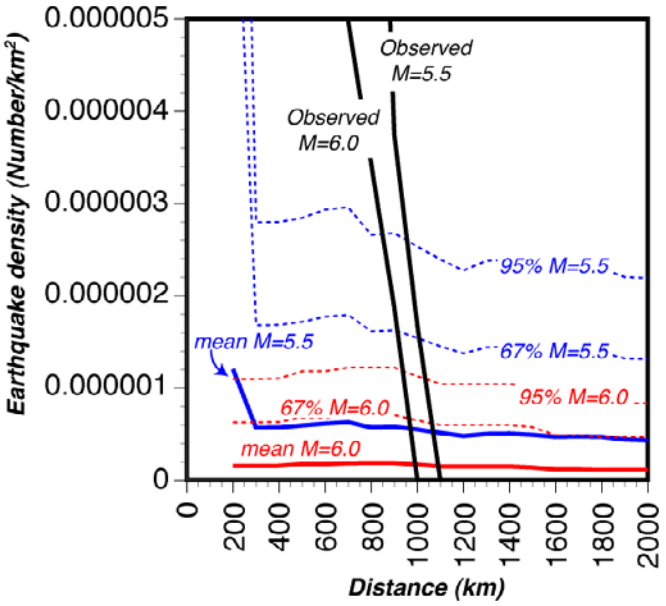

Figure S2. Observed 5.5<*M*<7 and 6≤*M*<7 earthquake density vs. distance. Black curves show earthquake density vs. distance from mainshocks over 50 minutes (same analysis as in Figure 2 except with higher completeness thresholds). The blue curves show mean background rates vs distance from triggering sources and confidence bounds for 5.5<*M*<7 events, and the red curves show the same information for 6≤*M*<7 earthquakes. Anomalously high observed rates are observed at distances where the black curves are higher than background rates, which is less than 900-1100 km for *M*≥ 6.0 and *M*≥5.5 events respectively.

Supplementary References

Cao, A. M., and S. S. Gao (2002), Temporal variation of seismic b-values beneath northeastern Japan island arc,, Geophys. Res. Lett. 29, doi 10.1029/2001GL013775.

Ringdal, F. (1986), Study of magnitudes, seismicity, and earthquake detectability using a global network, Bull. Seismol. Soc. Am., 76, 1641-1659.

Shi, Y., and B. A. Bolt (1982), The standard error of the magnitude frequency b-value, Bull. Seism. Soc. Am. 72, 1677–1687.

Wiemer, S., and M. Wyss (2000), Minimum magnitude of complete reporting in earthquake catalogs: examples from Alaska, the Western United States, and Japan, Bull. Seism. Soc. Am. 90, 859–869.

Woessner, J., and S. Wiemer (2005), Assessing the quality of earthquake catalogues: Estimating the magnitude of completeness and its uncertainty, Bull. Seismol. Soc. Am., 95, 684–698, doi: 10.1785/0120040007.